Communication

Sensitivity-enhanced Experiments for the Measurement of *J* and Dipolar Coupling Constants

LIN, Dong-Hai[*,a](林东海) **LIAO, Xin-Li**[b](廖新丽)

[a] *Department of Biochemistry, The Hong Kong University of Science & Technology, Hong Kong, China*

[b] *Department of Chemistry, Xiamen University, Fujian 361005, China*

A sensitivity-enhanced IPAP NMR experiment was described in this paper, which separates the ^{1}H-^{15}N doublets into two different spectra to alleviate the problem of resonance overlaps and achieve the accurate measurement of *J* and residual dipolar coupling constants in proteins. This experiment offered 20%—60% sensitivity enhancement over the original IPAP experiment, and therefore produced more measurable resonances. Pulsed field gradient was used for coherence selection. Water-flip-back approach was used for water suppression. The sensitivity-enhanced IPAP experiment was employed in the measurement of $^1J_{NH}$ and $^1D_{NH}$ constants of the protein UBC9.

Keywords *J* coupling, residual dipolar coupling, liquid crytalline media, spin-state separated spectra, sensitivity enhancement

Residual dipolar coupling constants provide information about the orientations of internuclear vectors, which are long range structural constraints and are complementary to the short range restraints obtained from nuclear Overhauser effects and vicinal *J*-coupling constants.[1-4] The residual dipolar coupling constants, $^1D_{NH}$, can, in principle, be measured from a HSQC (Heteronuclear single quantum coherence) spectrum without ^{1}H-decoupling in the t_1 dimension. However, since each peak splits into a doublet, resonance overlaps become more severe and can prevent accurate measurements for many residues. Recently, Bax and co-workers provided an elegant approach to perform these measurements.[5] In this approach, two spectra were generated, which contained the upfield components and the downfield components of ^{15}N doublets, respectively. These two spectra were obtained by addition and subtraction of two other spectra which corresponded to the inphase (IP) and antiphase (AP) ^{15}N doublets, respectively. This approach was referred to as the IPAP approach. Specifically, a regular ^{1}H-coupled [^{15}N, ^{1}H] HSQC experiment was carried out to generate inphase ^{15}N doublets in the t_1 dimension. A second ^{1}H-^{15}N correlation experiment was carried out to generate antiphase (AP) ^{15}N doublets in the t_1 dimension by inserting an ^{15}N refocusing period $\Delta \approx 1/(2\,^1J_{NH})$ before t_1 evolution. After optimum scaling of the signals in the second spectrum to compensate for signal loss during period Δ and the variations in $^1J_{NH}$, the two spectra were added and subtracted to generate two other spectra which contained the upfield and the downfield components of ^{15}N doublets, respectively. In these experiments, two orthogonal terms, $2I_zS_y$ and $2I_zS_x$ ($I = {}^1H$, $S = {}^{15}N$), were generated from the t_1 evolution under the chemical-shift Hamiltonian. However, only one term was refocused, and thus sensitivity of the experiments were not optimal.

In this paper, we describe an approach to preserve both terms, $2I_zS_y$ and $2I_zS_x$, in the IPAP method to enhance sensitivity. Pulsed field gradient (PFG) was used for coherence selection, sensitivity enhancement, and water suppression, based on the approach developed previously by Rance, Kay, and co-workers, which is also known as PEP (peservation of equivalent pathways).[6-9] It was showed that spectra can be generated which correspond to the upfield or downfield components of the ^{15}N doublets with sensitivity-enhancement, and accurate measurement of *J* and residual dipolar coupling constants is achieved.

* E-mail: donghail@ust.hk; Tel: 852-23588785; Fax: 852-23581716

Received December 12, 2001; revised and accepted May 15, 2002.

Project supported by the National Natural Science Foundation of China (No. 19975038).

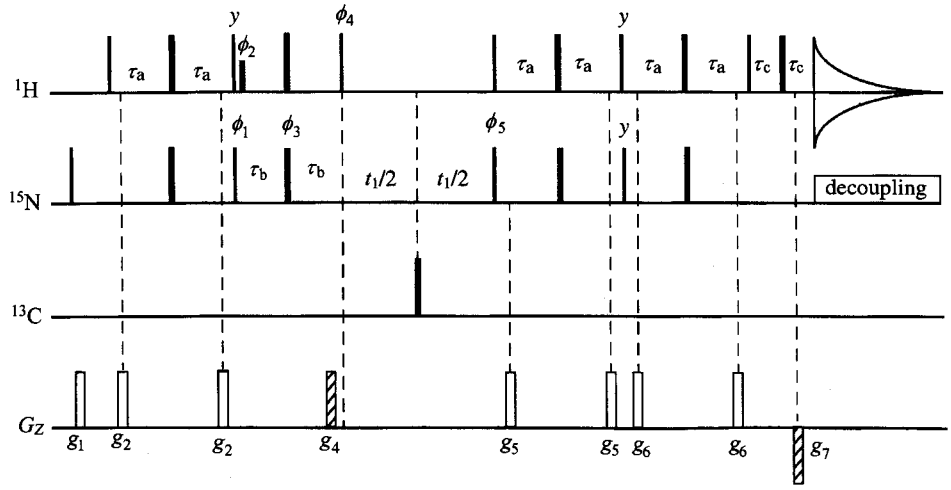

Fig. 1 Pulse scheme of sensitivity-enhanced IPAP experiment. Narrow and wide pulses correspond to 90° and 180° pulses, respectively. The phases of these pulses are x, unless indicated otherwise. The 180°(^{1}H) pulse applied at the center of the $2\tau_b$ period is only used in the experiment for generating the antiphase spectrum. The $90°_{\phi 4}$(^{1}H) pulse is used to eliminate the dispersive components in the ^{15}N dimension. This 90° pulse and the 180°(^{1}H) pulse at the center of the $2\tau_b$ period are omitted in the IP experiment. The water-flip-back approach is employed to minimize saturation/dephasing of water and eliminate water signal. The water selective $90°_{\phi 2}$ pulse is only used in the IP experiment. The delay τ_a, τ_b and τ_c were 2.5, 2.5 and 0.5 ms. A 180°(^{13}C) pulse is applied for decoupling during t_1 with the carrier placed at the center of $^{13}C_\alpha$ and ^{13}CO resonances. Phase cyclings are: $\phi_1 = y$, $\phi_4 = -x$ for the AP experiment, $\phi_1 = x$, $\phi_2 = x$ for the IP experiment; $\phi_3 = (x, y, -x, -y, -x, -y, x, y)$, $\phi_5 = x$, receiver = $(x, -x)$. The phase of ϕ_5 is inverted when the phase of the gradient pulse g_7 is reversed for quadrature detection. The phase of ϕ_1 is increased by 180° along with the phase of receiver for each increment of t_1.

The pulse scheme is shown in Fig. 1. In order to obtain both the inphase and antiphase ^{15}N doublets, the delay $2\tau_b$ is placed in front of the t_1 evolution period. Coherence selection is obtained by using two gradient pulses, g_4 and g_7. Most Hamiltonians during the $2\tau_b$ duration and the t_1 evolution period commute with each other. The only terms that do not commute with the Hamiltonian for the t_1 evolution are the Hamiltonians for 180° (^{15}N) and the 180° (^{1}H) pulses in the duration $2\tau_b$, which inverts the M_x, M_y or M_z of ^{15}N and ^{1}H spins. To compensate for the inversion of the ^{15}N magnetization, the sign of the gradient pulse g_7 is inverted also. Therefore, placing the $2\tau_b$ period in front of the t_1 evolution does not affect coherence selection. The gradient pulse, g_4, in addition to coherence selection, also dephases and suppresses the residual transverse magnetization of water prior to the t_1 evolution period. In the conventional gradient-enhanced HSQC pulse sequence,[9] this is achieved by an additional gradient pulse, g_3, between the 90° (^{1}H) pulse and the 90° (^{15}N) pulse at the end of the first INEPT step. In these experiments, there is not a significant increase in the delay lengths; only τ_b is increased from 1.5 ms in the gradient-enhanced HSQC to 2.5 ms [$\sim 1/(4\,{}^1J_{NH})$] in our experiments. The $^1J_{NH}$ coupling constants are measured in the ^{15}N dimension. The water-flip-back approach[10] is employed to minimize saturation/dephasing of water and eliminate water signal.

In this approach, the first experiment generates antiphase ^{15}N doublets in the F_1 dimension (^{15}N). Since the duration τ_b is set to $1/(4\,{}^1J_{NH})$, the duration $\tau_b - 180°_x(^{15}N), 180°_x(^1H) - \tau_b$ acts as an ^{15}N refocusing period, converting the antiphase coherence, generated at the end of the first INEPT step, into an inphase ^{15}N coherence. A $90°_{\phi 4}$(^{1}H) pulse is added at the end of the $2\tau_b$ period to eliminate the dispersive components, which result from τ_b not being $1/(4\,{}^1J_{HN})$ for some residues. The observable density operator immediately prior to the t_2 acquisition ($t_2 = 0$) is given by Eq. (1),

$$\sigma(\mathrm{AP},\ 1) = [I_x\cos(\omega_S t_1) + I_y\sin(\omega_S t_1)](1/2)\cdot (\varepsilon_I + \varepsilon_{MQ})\sin(\pi J_{NH} t_1) \qquad (1)$$

where the factors $\varepsilon_I = \exp(-2R_{1I}\tau_a)$, $\varepsilon_{MQ} = \exp(-2R_{2MQ}\tau_a)$, R_{1I} is the longitudinal relaxation rate constant of ^1H spins, and R_{2MQ} the transverse relaxation rate constant for heteronuclear multiple-quantum coherences. In order to separate the two orthogonal components, a second experiment was performed in which the phases of the $90°_{\phi5}(^{15}N)$ pulse and the sign of gradient pulse g_7 are inverted. The observable density operator at $t_2 = 0$ is given by Eq. (2),

$$\sigma(AP, 2) = [I_x\cos(\omega_S t_1) - I_y\sin(\omega_S t_1)](1/2)\cdot (\varepsilon_I + \varepsilon_{MQ})\sin(\pi J_{NH} t_1) \quad (2)$$

The sine- and cosine-modulated terms that result from addition and subtraction of the acquired data sets shown in Eqs. (1) and (2) are given by Eqs. (3) and (4),

$$\sigma(AP, x) = I_x\cos(\omega_S t_1)(\varepsilon_I + \varepsilon_{MQ})\sin(\pi J_{NH} t_1) \quad (3)$$

$$\sigma(AP, y) = I_y\sin(\omega_S t_1)(\varepsilon_I + \varepsilon_{MQ})\sin(\pi J_{NH} t_1) \quad (4)$$

The second experiment, the IP experiment, was carried out to generate inphase doublets in the F_1 dimension. In this experiment, the $180°(^1H)$ in period $2\tau_b$ is omitted and the phase of $90°_{\phi1}(^{15}N)$ pulse is decreased by 90° compared to the first experiment. Thus the antiphase coherence, $-2I_zS_y$ is kept as an antiphase coherence during the $2\tau_b$ period. Similar to the AP experiment, the sine- and cosine-modulated terms that result from addition and subtraction of the acquired data sets are given by Eqs. (5) and (6),

$$\sigma(IP, x) = -I_x\sin(\omega_S t_1)(\varepsilon_I + \varepsilon_{MQ})\cos(\pi J_{NH} t_1) \quad (5)$$

$$\sigma(IP, y) = I_y\cos(\omega_S t_1)(\varepsilon_I + \varepsilon_{MQ})\cos(\pi J_{NH} t_1) \quad (6)$$

The addition and subtraction of the IP and AP experiments give Eqs. (7) and (8),

$$\sigma(IP + AP, x) = -I_x\sin(\omega_S t_1 \mp \pi J_{NH} t_1)(\varepsilon_I + \varepsilon_{MQ}) \quad (7)$$

$$\sigma(IP + AP, y) = I_y\cos(\omega_S t_1 \mp \pi J_{NH} t_1)(\varepsilon_I + \varepsilon_{MQ}) \quad (8)$$

which show that the two orthogonal components have identical magnitudes and can be treated as a hypercomplex quadrature pair in the t_1 dimension after a 90° zero-order phase correction. Fourier transformation of the data yield spectra with signals at either $\omega_S - \pi J_{NH}$ or $\omega_S + \pi J_{NH}$ in the F_1 dimension.

The signal loss during the $2\tau_b$ period for both the IP and AP experiments is very similar. The signal loss mainly results from ^{15}N transverse relaxation, imperfections of the two 180° pulses applied at the center of the $2\tau_b$ period, and the variations in $^1J_{HN}$. The two factors, imperfections of the 180° pulses and variations in $^1J_{NH}$, should affect both experiments similarly. For both IP and AP experiments, ^{15}N transverse relaxation rates during the $2\tau_b$ period are similar and are the averages of the transverse relaxation rates of the inphase and antiphase coherences.[11,12] The only factor which affects the two experiments differently is the interference between the ^{15}N chemical shift anisotropy (CSA) and ^{15}N-^1H dipolar coupling. For the AP experiment, cross-correlation has no net effect on the relative signal intensities of the two ^{15}N doublets, because the spin-state of amide proton is inverted at the center of the $2\tau_b$ period.[13] However, in the IP experiment, the two ^{15}N doublets relax at different rates as a result of cross-correlation, and therefore have relative intensities of $\exp(2\eta\tau_b)$ and $\exp(-2\eta\tau_b)$, respectively, where η is the relaxation rate constant due to cross-correlation.[13] At 500 MHz the theoretical value of η is 35% of the inphase ^{15}N transverse relaxation rate R_2.[13] The average R_2 of UBC9 is approximately 15 s^{-1}.[14] Therefore $\exp(4\eta\tau_b)$ is approximately 1.05 for most residues. This theoretical estimate was confirmed experimentally. We compared the relative peak intensities of the upfield components and the downfield components between the sensitivity-enhanced IP experiment and the F_1-coupled HSQC to estimate the effect of cross-correlation. Relaxation due to η (*e.g.* $\exp(4\eta\tau_b)$) caused approximately 5%—10% changes in the relative peak intensities in the sensitivity-enhanced IP experiment. When the concentration of UBC9 is about 0.5—1 mmol·L^{-1}, these differences in intensity are comparable to the noise level of the spectra (about 5%—10% of the peak intensity). Therefore, addition and subtraction of the IP and AP spectra produced clean spin-state-separated spectra and "ghost" peaks were not visible.

This method was used to measure the J coupling constants ($^1J_{NH}$) and the residual dipolar coupling con-

stants ($^1D_{NH}$) in a 0.5 mmol·L^{-1} sample of ^{15}N-labeled UBC9, in 100 mmol·L^{-1} sodium phosphate buffer, pH 6.0, in 90% H_2O/10% D_2O. Resonance assignments of UBC9 have been described previously.[15] The solution contained either no lipid or 5% lipid composed of dilauryl phosphatidylcholine (DLPC) and 3-(cholamidopropyl) dimethylammonio-2-hydroxyl-1-propane sulfonate (CHAPSO) in a 4.2∶1 molar ratio.[16] All spectra were recorded on a Varian UNITY plus 500 NMR spectrometer at 25 ℃. Fig. 2 shows regions of the sensitivity-enhanced IPAP spectra of UBC9, recorded in the liquid crystalline medium, using the pulse scheme shown in Fig. 1. Fig. 2A displays the downfield components of ^{15}N doublets, and Fig. 2B, the upfield components. Fig. 3 presents 1 D slices of the peaks of a typical residue (D100) of UBC9 in these and the corresponding spectra of the original IPAP experiment.[5] Sensitivity enhancement of factors from 1.2 to 1.6 was observed for the measurable residues in the sensitivity-enhanced IPAP spectra.

The lipid system appears to take hours to reach stable alignment state. For the few samples that we made using this lipid (DLPC/CHAPSO) system, we noticed that the splitting of the deuterium signal continued to increase over a few hours after placed in the magnet and can increase as much as 1.5 Hz overnight. Therefore, all of the experiments were started after the sample was in the magnet overnight.

Accuracy of the measurements using the sensitivity-enhanced IPAP approach was examined . The $^1J_{NH}$ + $^1D_{NH}$ coupling constants were measured for 48 resolved residues of UBC9 in liquid crystalline state by using the sensitivity-enhanced IPAP experiment, the ^{1}H-coupled [^{15}N, ^{1}H] HSQC experiment,[9] and the original IPAP experiment.[5] For 11 of the 48 residues, the coupling constants measured from the ^{1}H-coupled [^{15}N, ^{1}H] HSQC experiment and those measured from the sensitivity-enhanced IPAP experiment show differences larger than the digital resolution. However, the coupling constants of 8 of the 11 residues measured from the original IPAP experiment and the sensitivity-enhanced IPAP experiment are similar and the differences are within the digital resolution. Three other residues show large errors among the three measurements. Since the accuracy of the original IPAP experiment has been assessed previously, these errors are likely due to instability of UBC9 in the lipid system composed of DLPC and CHAPSO, and not due to the method itself. Fig. 4 shows the residual dipolar coupling constants of UBC9 measured from the sensitivity-enhanced IPAP spectra versus those measured from F_1-doublets of a ^{1}H-coupled [^{15}N, ^{1}H] HSQC spectra and the original IPAP spectra.

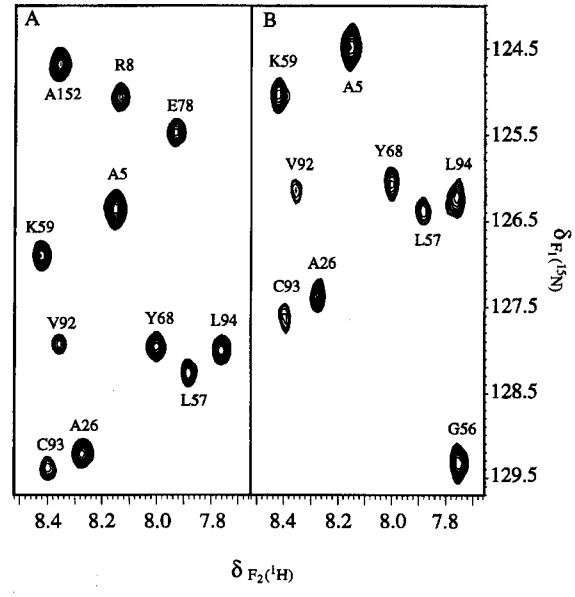

Fig. 2 (A) and (B) show a region of the sensitivity-enhanced IPAP spectra recorded in the dilute liquid crystalline medium at 25 ℃. Peaks in (A) are the downfield components and in (B) the upfield components of ^{15}N doublets, obtained by subtracting and adding the IP and AP spectra recorded with the pulse scheme shown in Fig. 1. The strength and duration of gradient pulses were g_1 = (1.0 ms, 8 G/cm), g_2 = (0.5 ms, 8 G/cm), g_4 = (1.25 ms, 30 G/cm), $g_5 = g_6$ = (0.15 ms, 15 G/cm), g_7 = (0.125 ms, 28.9 G/cm).

The sensitivity-enhanced IPAP experiment records more measurable resonances. For UBC9, totally, 57 residual dipolar coupling constants ($^1D_{NH}$) were measured from the resolved resonances in the sensitivity-enhanced IPAP experiment, whereas only 48 residual dipolar coupling constants were measured from the resolved resonances in the original IPAP experiment as some resonances has intensities close to the noise level.

In conclusion, the sensitivity-enhanced IPAP experiment produces clean spin-state separated spectra each containing only the upfield or the downfield components of ^{15}N doublets. This experiment has significantly higher sensitivity and much better water suppression due to the use of gradient for coherence selection. Therefore, more

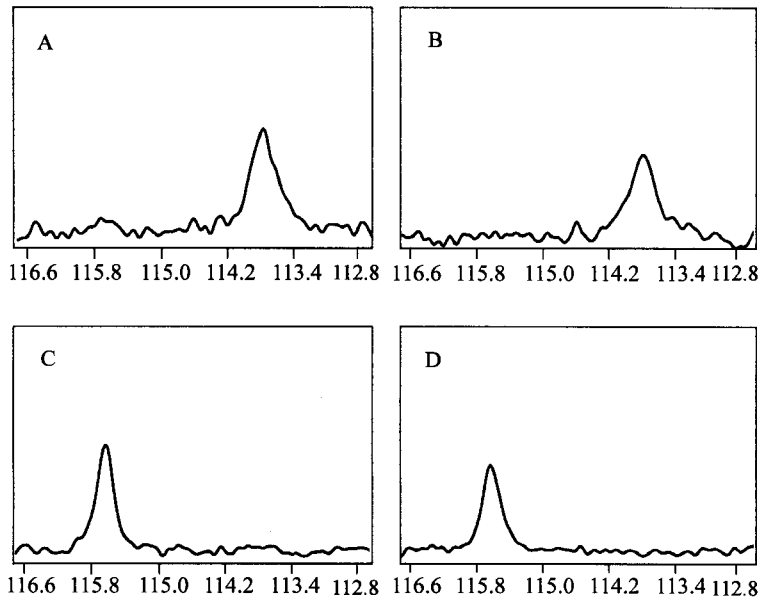

Fig. 3 Plots to demonstrate the sensitivity enhancement obtained in the sensitivity-enhanced IPAP experiment over the original IPAP experiment. (A) and (C) are the 1 D slices of the peaks of a typical residue (D100) of the protein UBC9 in the sensitivity-enhanced IPAP spectra shown in Figs. 2A and 2B, respectively. (B) and (D) are those of the same peaks in the original IPAP spectra. Sensitivity enhancement of factors 1.3 and 1.6 was observed for the peaks in (A) and (C), respectively. The same experimental and processing parameters were used to produce all spectra.

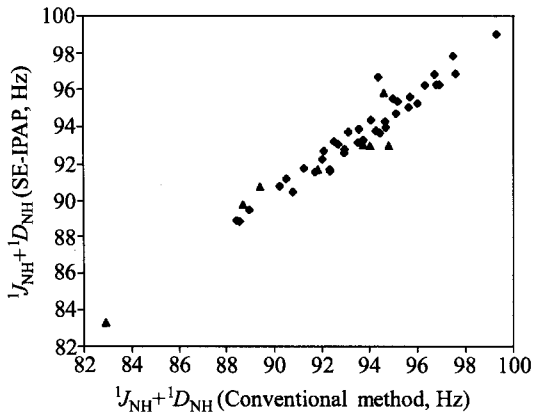

Fig. 4 $^1J_{NH} + ^1D_{NH}$, measured from the sensitivity-enhanced IPAP spectra versus those measured from F_1-doublets of a ^{1}H-coupled HSQC spectrum (solid squares) and from the original IPAP spectra (triangles). These measurements were done on ^{15}N-labeled UBC9 in the liquid crystalline medium at 25 ℃. The pairwise RMS (Root mean square) deviation is 0.7 Hz.

residues are measurable using this experiment than the original IPAP experiment. This approach can also be implemented in other heteronuclear NMR experiments to obtain residual dipolar coupling constants of other spin pairs. These dipolar coupling constants are important for accurate determination of three-dimensional structures of proteins, nucleic acids, and their complexes.

Acknowledgement

We would like to thank for the helpful discussion of Dr. Yuan Chen and Dr. Yeching Yuan.

References

1 Bothner-By, A. A., In *Encyclopedia of Nuclear Magnetic Resonance*, Eds.: Grant, D. M.; Harris, R. K., Wiley, Chichester, **1995**, pp. 2932—2938.

2 Tjandra, N.; Bax, A. *Science* **1997**, *278*, 1111.

3 Tjandra, N.; Omichinski, J. G.; Gronenborn, A. M.; Clore, G. M.; Bax, A. *Nat. Struct. Biol.* **1997**, *4*, 732.

4 Sanders, C. R.; Hare, B. J.; Howard, K. P.; Prestigard, J. H. *Prog. Nucl. Magn. Reson. Spectrosc.* **1997**, *26*, 421.

5 Ottiger, M.; Delaglio, F.; Bax, A. *J. Magn. Reson.* **1998**, *131*, 373.

6 Cavanagh, J.; Palmer, A. G.; Wright, P. E.; Rance, M. *J. Magn. Reson.* **1991**, *91*, 429.
7 Palmer, A. G.; Cavanagh, J.; Byrd, R. A.; Rance, M. *J. Magn. Reson.* **1992**, *96*, 416.
8 Kay, L. E.; Keifer, P.; Saarinen, T. *J. Am. Chem. Soc.* **1992**, *114*, 10663.
9 Zhang, O.; Kay, L. E.; Olivier, J. P.; Forman-Kay, J. D. *J. Biomol. NMR* **1994**, *4*, 845.
10 Grzesiek, S.; Bax, A. *J. Am. Chem. Soc.* **1993**, *115*, 12593.
11 Peng, J.; Wagner, G. *J. Magn. Reson.* **1992**, *98*, 308.
12 Boulat, B.; Bodenhausen, G. *J. Biomol. NMR* **1993**, *3*, 335.
13 Goldman, M. *J. Magn. Reson.* **1984**, *60*, 437.
14 Liu, Q.; Yuan, Y. C.; Shen, B.; Chen, D. J.; Chen, Y. *Biochemistry* **1999**, *38*, 1415.
15 Liu, Q.; Shen, B.; Chen, D. J.; Chen, Y. *J. Biomol. NMR* **1999**, *13*, 89.
16 Wang, H.; Eberstadt, M.; Olejniczak, E. T.; Meadows, R.; Fesik, S. W. *J. Biomol. NMR* **1998**, *12*, 443.

(E0112126 ZHAO, X. J.)